Available online at www.sciencedirect.com
SCIENCE DIRECT®
International Journal of Thermal Sciences 45 (2006) 103–109
International Journal of Thermal Sciences
www.elsevier.com/locate/ijts

Radiative heat transfer for irregular geometries with the collapsed dimension method

Prabal Talukdar *

Institute of Fluid Mechanics, University of Erlangen-Nuremberg, Cauerstrasse 4, 91058 Erlangen, Germany

Received 19 April 2005; received in revised form 21 June 2005; accepted 21 June 2005

Available online 3 August 2005

Abstract

A blocked-off region procedure is implemented with the collapsed dimension method (CDM) to deal with radiative transport problems in irregular geometries. Different test problems are validated for radiative and non-radiative equilibrium situations in participating or non-participating media. Results are found to be satisfactory for all straight edged, inclined and curved boundaries. The blocked-off region procedure based on Cartesian coordinate is found to be very convenient for a ray-tracing method like the CDM. The same ray tracing algorithm for a rectangular enclosure could be effectively used for any kind of 2-D geometries. This significantly reduces the effort of developing different ray-tracing algorithm for different geometries. In addition, it is an alternative than to write an algorithm in curvilinear coordinate for irregular geometries which found to be complicated for a ray-tracing method like the CDM.

Keywords: Collapsed dimension method; Blocked-off region; Radiation; Participating media; Irregular geometry

1. Introduction

The popularity and usefulness of a method basically lies in its implementation to real geometries. Almost all the real geometries are irregular and complex in nature and is the reason for ever increasing trend of research in radiative heat transfer for complicated geometries. It has also become a challenge for a particular method as far as its applicability and accuracy with the irregular structures are concerned.

Most of the papers dealing with the irregular geometries for radiative transport are found in the 90's. Sanchez and Smith [1] used the discrete ordinates method for surface radiative exchange between the faces of geometries with straight edged protrusions and obstructions. Chai et al. [2,3] simulated radiative transfer in irregular geometries using the discrete ordinates method [2] and the finite volume method [3]. They used a similar blocked-off region procedure to simulate the irregularities based on Cartesian coordinate. They found satisfactory results and discussed the advantages and disadvantages found with this procedure. Koo et al. [4] studied the effect of three different discrete ordinates methods applied to 2-D curved geometries. In another paper, Koo et al. [5] discussed the first order and second order interpolation schemes in context with the irregular geometries. Monte Carlo method has been applied by Parthasarathy et al. [6] for irregular geometries. They considered a rhombus, a quadrilateral and an enclosure with curved and straight edged boundaries. They considered absorbing, emitting and anisotropically scattering medium. Sakami and Charette [7] discussed a modified discrete ordinates method based on triangular grids with a new differencing scheme applicable to different complex geometries. Some works for 2-D irregular geometries has been done by Meng et al. [8] using the discrete transfer method with a finite element formulation. Some of the papers are also devoted to 3-D irregular geometries. Malalasekera and James [9] implemented the discrete transfer method to a 3-D L-shaped enclosure and a cylindrical enclosure based on a non-orthogonal, body-fitted coordinate system.

* Tel.: 0049 9131 8529 489; fax: 0049 9131 8529 503.
E-mail address: prabal_iitg@yahoo.com (P. Talukdar).

1290-0729/$ – see front matter
doi:10.1016/j.ijthermalsci.2005.06.006

Nomenclature

I	intensity	$W{\cdot}m^{-2}{\cdot}sr^{-1}$
M	total number of intensities/rays	
p	phase function	
q	heat flux	$W{\cdot}m^{-2}$
S	source function	$W{\cdot}m^{-2}$
T	temperature	K
T_g	temperature of the isothermal medium	K
T_h	temperature of the hot boundary	K

Greek symbols

α	planar angle	rad
$\Delta\alpha$	angular thickness of the discrete planar angle	rad
β	extinction coefficient	m^{-1}
η	collapsing coefficient	
ε	emissivity	
σ	Stefan–Boltzmann constant	$W{\cdot}m^{-2}{\cdot}K^{-4}$
τ	optical thickness/depth	
ω	scattering albedo	

Subscripts

ref	reference
w	boundary/wall

Malalasekera and Lockwood [10] also used the discrete transfer method in conjunction with a cell-blocking procedure based on Cartesian coordinate to model combustion and radiative heat transfer in complex three-dimensional tunnel geometry.

The CDM is one of the new methods emerging out in radiative transfer problems with participating and non-participating medium. The method is tested for different situations [11,12] and found to be satisfactory. It is accurate and also economical for a 2-D problem [12]. The method is also implemented for complex geometries [13] for limited cases of non-radiative equilibrium situation. A separate ray-tracing algorithm was developed for cylindrical, L-shaped and quadrilateral geometries. Due to the complexities associated with the radiative equilibrium situation for these type of geometries, it was not implemented for those situations. Even for non-radiative equilibrium, its ray tracing was quite tedious depending on the shape of the geometries. The biggest disadvantage suffered by this method was the non-availability of a single algorithm which can handle any kind of geometries. The present blocked-off region approach extends the applicability of the CDM and makes it more general in radiative transport problems in participating medium.

The concept of blocked-off region for radiation was first implemented by Chai and his co-workers for the finite volume method [3] and the discrete ordinates method [2]. They validated the results for different test problems and discussed the advantages and disadvantages of this approach.

The implementation of the blocked-off region approach to the CDM is very straightforward. Although conceptually it is similar to the work of Chai et al. [2], as far as its implementation is concerned, it has a different approach which is quite simple. A whole rectangular domain which can be called as a nominal or simulated domain is simulated, out of which one portion is considered to be inactive or blocked-off and the remaining portion is the actual domain where solutions are sought. As soon as an intensity travels through these inactive regions, its value becomes zero. The tedious part of ray tracing is only once developed for a 2-D rectangular geometry and can be successfully implemented to different irregular geometries by dividing the domain into inactive and active sub domains. Five different test problems are considered to check its accuracy and applicability. The CDM fully enjoys this new concept and presents satisfactory results.

2. Analysis

Radiative transfer in irregular geometries is treated with a concept used in CFD [14]. The algorithm written for a regular grid can be modified to handle an irregularly shaped calculation domain. This is done by making some of the control volumes of the regular grid inactive or blocked-off so that the remaining active control volumes represent the desired irregular domain.

Two sample geometries are shown in Fig. 1. The real domain of interest is calculated by considering the whole rectangular domain mentioned as simulated domain. The shaded portion is the inactive or blocked off region where solutions are not required. In Fig. 1(b), a curved boundary is shown which can also be handled by this concept with the step size grid. This way any type of 2-D geometry can be modelled from a rectangular domain. The main advantage achieved with this concept is that the same ray tracing algorithm can be applied to any kind of irregular structures with a little expense of computational time.

The CDM [15] is a ray tracing method. To calculate flux or incident radiation at a certain location, intensities from all directions α $(0 \leqslant \alpha \leqslant 2\pi)$ [11,15] have to be calculated. In the CDM, the intensities are always traced from the boundaries. If the boundary temperature is known, intensities at the boundary can be calculated from the relation,

$$I_w = \frac{\varepsilon_w \sigma T_w^4}{2} + \frac{1-\varepsilon_w}{2} \int_{\alpha=0}^{\pi} I^-(\alpha) \sin\alpha \, d\alpha \tag{1}$$

On the right-hand side, the first term in the above equation is the emitted part and the second term is the reflected part

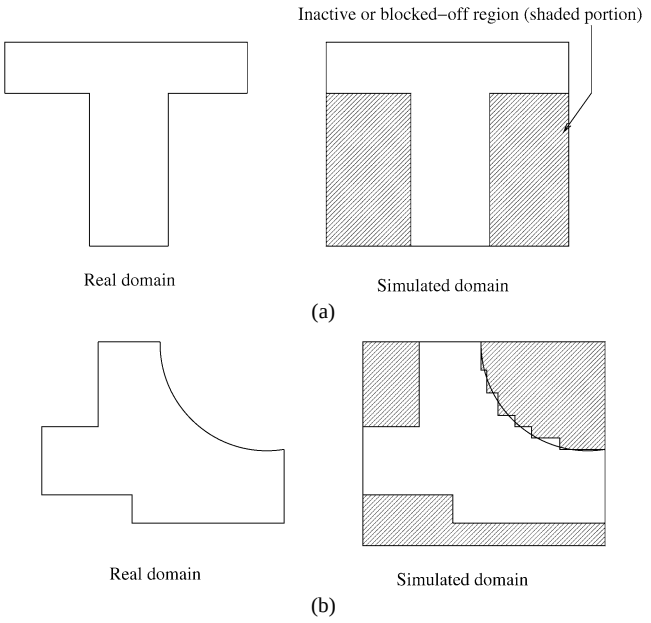

Fig. 1. Sample irregular geometries.

for a diffuse gray boundary. In this equation, T_w is the temperature of the boundary and I^- is the incoming intensity to the boundary, part of which is reflected back to the medium. Once boundary intensity is known, the intensities are traced step by step through the control volumes. The recursive relation to calculate the intensity at a point $n+1$ from the known intensity at point n is given by

$$I_{n+1} = I_n \exp(-\tau\eta) + S\big[1 - \exp(-\tau\eta)\big] \tag{2}$$

Here S is the source function known or evaluated from the previous intensity distribution in an iterative process. τ and η represent respectively the optical thickness of the medium and the collapsing coefficient for the CDM. The discussions about collapsing coefficient for the CDM can be found in [15]. In this work, the source function in a particular control volume is different for different intensities and are calculated with the bilinear interpolation of the source function values at the four corners of a particular control volume.

The source function in a particular direction α is calculated as

$$S = \frac{(1-\omega)\sigma T^4}{2} + \frac{\omega}{2\pi}\int_{\alpha'=0}^{2\pi} I(\alpha')\,p(\alpha' \to \alpha)\,\mathrm{d}\alpha' \tag{3}$$

where ω, T and p are the scattering albedo, temperature of the medium and the phase function, respectively. In the present work, only isotropic scattering is considered and hence, the value of p is taken to be 1. The angle α defines the direction of an intensity measured from normal to the control surface.

Once intensity distributions are known, the radiative heat flux at a particular location can be calculated by integrating

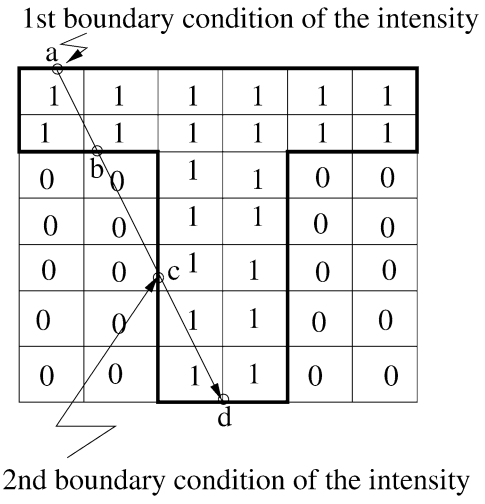

Fig. 2. Ray tracing in a domain with a blocked-off/inactive region.

the intensities over complete span of ($0 \leqslant \alpha \leqslant 2\pi$) and can be expressed as

$$q = \int_{\alpha=0}^{2\pi} I(\alpha)\sin\alpha\,\mathrm{d}\alpha \tag{4}$$

This can be numerically integrated as

$$q = \sum_{n=1}^{M} c_n I(\alpha_n) \tag{5}$$

where in general

$$c_n = \left|\cos\left(\alpha_n + \frac{\Delta\alpha_n}{2}\right) - \cos\left(\alpha_n - \frac{\Delta\alpha_n}{2}\right)\right| \tag{6}$$

In Eq. (5), M is the number of intensities spanned over $0 \leqslant \alpha \leqslant 2\pi$ and in Eq. (6), $\Delta\alpha_n$ is the discrete planar angle over which nth intensity is assumed constant. In the present case, $\Delta\alpha_n$ is same for all intensities.

In the proposed blocked-off region procedure for the CDM, the domain is divided into two regions known as inactive or blocked-off and the real. As soon as an intensity passes through these inactive regions its magnitude becomes zero. The intensity takes a new boundary condition at the interface of inactive and real domain. In Fig. 2, how a domain is described for this problem is shown. This case is in reference to Fig. 1(a) of T-shaped enclosure. The whole simulated domain is discretised into several control volumes and the control volumes which are inside the active regions are designated as one (1) and otherwise they are zero (0). A typical intensity path ad is shown in this figure. The intensity originates from point a with a known boundary condition. As soon as the intensity passes through a point b, it enters to a zero domain. As a result, its history gets terminated and it becomes zero till it reaches the point c. At point c, which is at the interface between the inactive and active regions, it gets a second boundary condition. Calculations for the path ac is meaningless and only the cd path contributes to the flux calculations at point d.

For every type of geometry, a domain file has to be created as shown in Fig. 2. By changing the value of a control volume from 1 to 0, it can be made inactive. This domain file has to be created as per the grid file for a particular problem. The other important additional task for this approach is to define the additional boundary conditions referred as the second boundary condition in Fig. 2. Depending on the shape of the geometry, a boundary condition file has to be specified.

3. Results and validation

Five test problems are solved to show the performance of the CDM with the blocked-off region procedure. Except the last problem which deals with non-participating media, all other problems deals with participating media. Both radiative and non-radiative equilibrium situations are considered. Test Problems 1 and 2 are self validated and the others are compared with the literature. For all problems considered, boundaries are assumed to be black although the work has no limitation to gray boundaries.

Test Problem 1. The first problem considered is a problem with radiative equilibrium. The real geometry is extended by $0.5d$ in the left side and then simulated by making the extended portion as an inactive region. This clearly validates the applicability and accuracy of the blocked-off region. In Fig. 3(a), the description of the geometry is given. The left figure is the real geometry with left boundary at temperature $T = 0.5T_h$, bottom boundary at $T = T_h$ and the other two boundaries at $T = 0$. The simulated geometry is shown in the right side of Fig. 3(a) with the blocked-off region shown by the shaded portion. Calculations are performed for both the real geometry and the simulated geometry separately and compared in Fig. 3(b) and (c). In both cases (real and simulated), equal number of rays (= 32) are considered. In Fig. 3(b), emissive power distributions, $(T/T_h)^4$ are shown along y-direction at $x/d = 0.5$ (in reference to

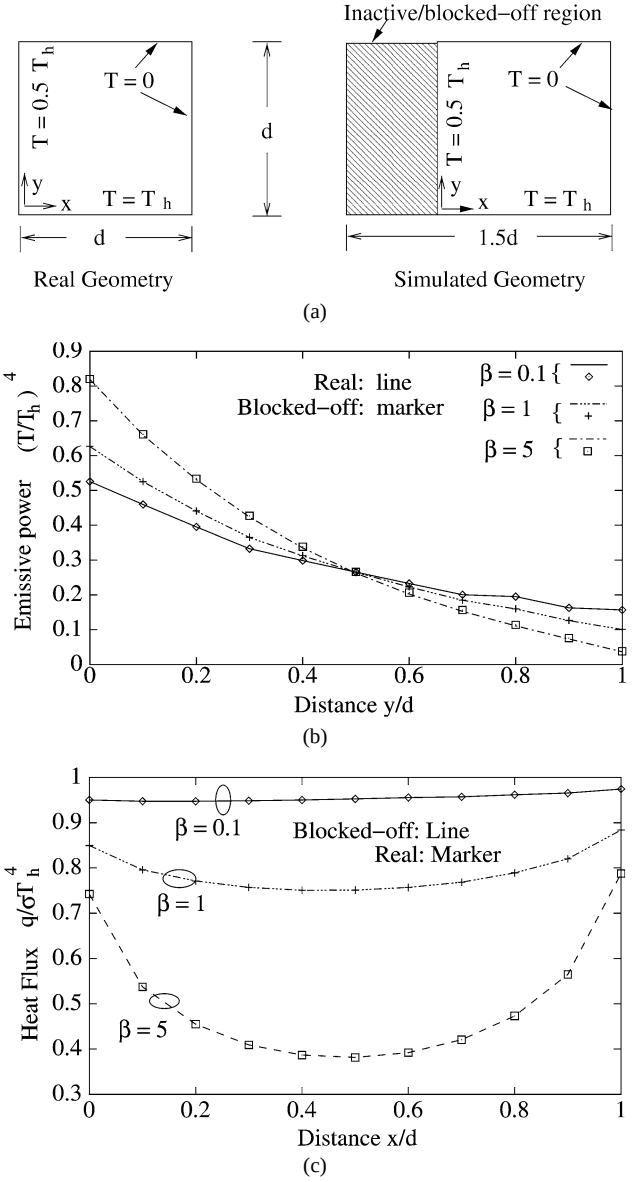

Fig. 3. (a) Sample geometry, (b) emissive power at $x/d = 0.5$, (c) heat flux at the bottom wall; radiative equilibrium.

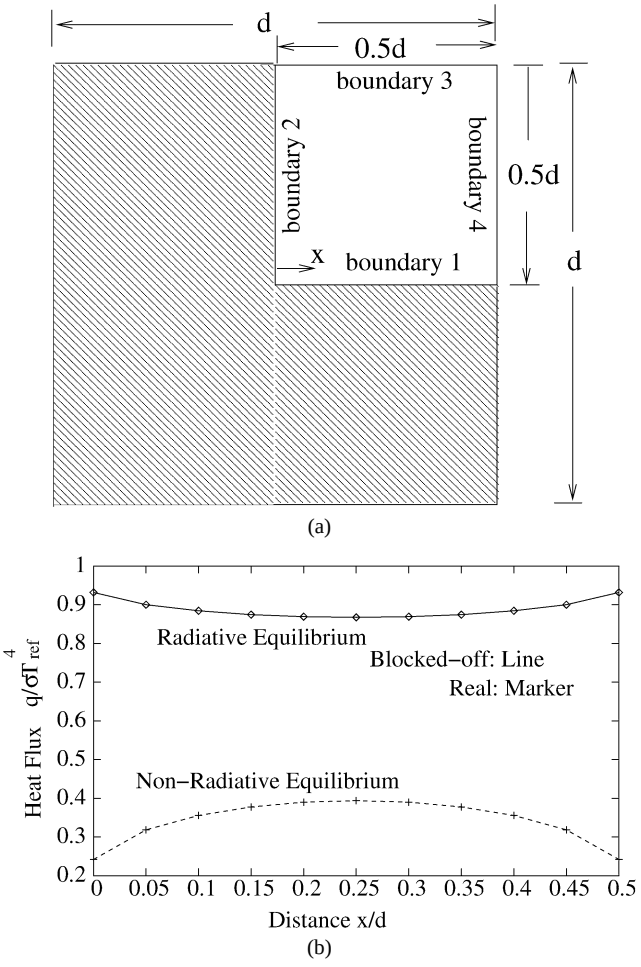

Fig. 4. (a) Sample geometry, (b) heat flux distributions at the boundary 1.

the real geometry configuration). Three different extinction coefficients viz. $\beta = 0.1$, 1 and 5 are considered. Since, the medium is at radiative equilibrium and only isotropic scattering is considered, results are independent of scattering albedo. Results of the simulated geometry exactly match with the real geometry results. In Fig. 3(c), heat fluxes $q/(\sigma T_h^4)$ at the bottom boundary are compared and found exactly same.

Test Problem 2. The 2nd problem considered is a similar one with a L-shaped blocked-off region (Fig. 4(a)). The active area where solutions are sought is the un-shaded portion. Calculations are performed once for the active region (the real geometry) alone and then for the whole portion (active and inactive together) as seen in the figure. Both radiative and non-radiative equilibrium conditions are considered. For the non-radiative equilibrium situation, medium is isothermal (T_g) and all boundaries are cold (zero temperature). For the radiative equilibrium situation, boundary 1 is at some finite temperature (T_h) whereas other 3 boundaries are cold. Extinction coefficient β is taken as unity for both the situations and the scattering albedo ω is taken as 0 for the non-radiative equilibrium situation. The heat flux $q/(\sigma T_{ref}^4)$ distributions at the boundary 1 is shown in Fig. 4(b). The reference temperature T_{ref} is the medium temperature T_g in the non-radiative equilibrium situation and temperature T_h of the boundary 1, in the radiative equilibrium situation. Number of rays considered is 32 for both real and simulated geometries. In this case also, results of the blocked-off region procedure match exactly with the real geometry results for both the radiative and the non-radiative equilibrium situations.

Test Problem 3. The third problem is a quadrilateral geometry previously considered by other researchers [5,6,16] for validation of irregular geometries. The geometry is described in Fig. 5(a). A non-radiative equilibrium situation is considered with an isothermal medium T_g and cold boundaries. Three different extinction coefficients are considered with an absorbing-emitting medium. The whole rectangle is simulated with the inclined planes approximated by step size grids. A grid of 40×30 in the $X \times Y$ directions and 32 intensity directions are found to be sufficient to have accurate results. The heat flux $q/(\sigma T_g^4)$ results at the bottom boundary is shown in Fig. 5(b). Results are compared with the exact results available in the literature [16]. An excellent agreement has been found for this problem.

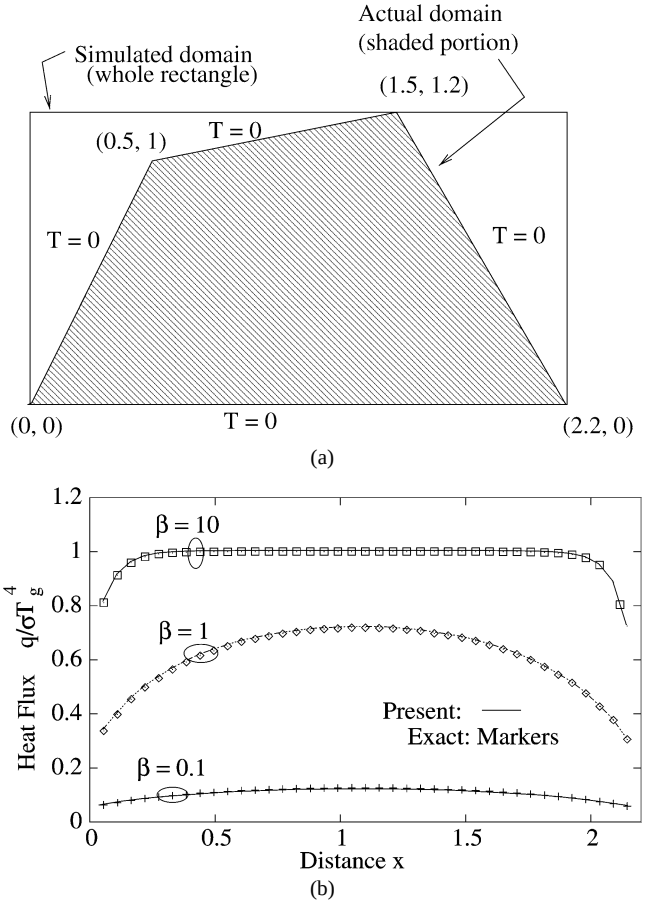

Fig. 5. (a) A quadrilateral geometry, (b) heat flux distributions at the bottom wall; non-radiative equilibrium.

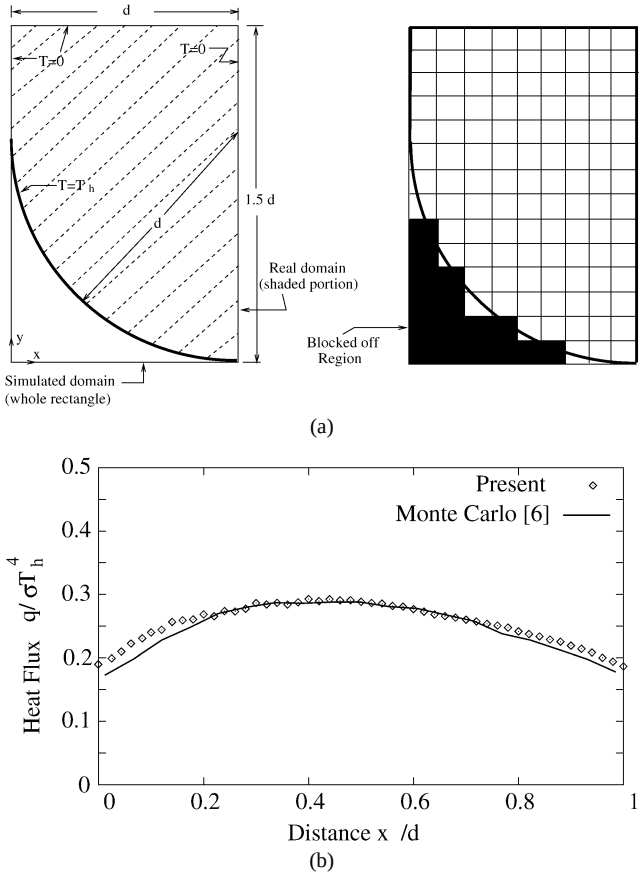

Fig. 6. (a) A curved geometry with step size grids, (b) heat flux distributions at the top boundary; radiative equilibrium.

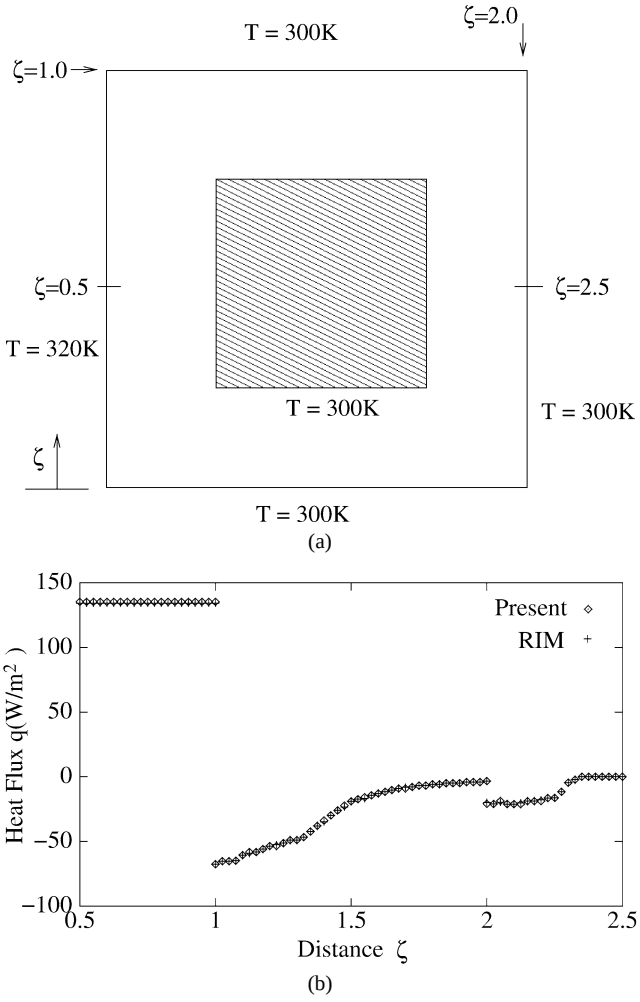

Fig. 7. (a) Schematic of the problem, (b) heat flux distributions at the enclosure wall; non-participating medium.

Test Problem 4. In the fourth problem, a geometry with a curved boundary is simulated. This geometry was previously solved by Chai and his co-workers [3,6,16] and Sakami and Charette [7]. The schematic of the problem is shown in Fig. 6(a). The curved boundary is simulated with a step size grid as shown in the figure. The actual grid considered is 30×50 $(X - Y)$ although in the figure a coarse grid is shown. This is a case of radiative equilibrium with the curved boundary at some finite temperature $T = T_{\mathrm{h}}$ while the other boundaries are cold $(T = 0)$. The extinction coefficient β of the medium is unity. The heat flux $q/(\sigma T_{\mathrm{h}}^4)$ results at the top boundary is shown in Fig. 6(b). The results of this work are found satisfactory as compared to the Monte Carlo results (taken to be exact) found in [6]. Although, the number of intensity directions considered here is quite high $(= 200)$ to reduce the ray effect at the cold top boundary, slight discrepancies at the edges could not be eliminated.

Test Problem 5. The last problem considered is the problem investigated previously by Sanchez and Smith [1] and then Chai et al. [3]. The schematic of the problem is shown in Fig. 7(a). It consists of a square enclosure with a central blockage. The medium is non-participating. The left boundary is set at 320 K and all the other boundaries including the boundaries of the central blockage are set at 300 K. The heat flux q results at the boundary of the enclosure are presented in Fig. 7(b). A total of 40×40 control volumes and 32 intensity directions are considered. The distance ζ is measured from the lower left corner of the enclosure. The results compare well with the solution of the RIM (radiosity/irradiation method) of Sanchez and Smith [1].

4. Conclusions and final remarks

This work shows that the CDM can be applied with the irregular geometries. The same Cartesian coordinate based algorithm can be applied to model curved and inclined boundaries and also can take care of blockages. This procedure is very advantageous for a ray tracing method like the CDM and shows quite accurate results. This procedure, of course, has the disadvantage of unnecessary calculation in the inactive region. In addition, a large number of control volumes have to be considered to model curved and inclined boundaries and calculation of flux and incident radiation on those boundaries are also difficult. But nevertheless, it shows an alternative as far as the tedious ray-tracing algorithm considered with the irregular geometries and hence can be considered as an useful approach for the solution of radiative transfer problems in irregular geometries with the CDM.

References

[1] A. Sanchez, T.F. Smith, Surface radiation exchange for two-dimensional rectangular enclosures using the discrete-ordinates method, J. Heat Transfer 114 (1992) 465–472.
[2] J.C. Chai, H.S. Lee, S.V. Patankar, Treatment of irregular geometries using a Cartesian coordinates control-angle, control-volume-based discrete-ordinates method, in: Proceedings of the National Heat Transfer Conference, American Society of Mechanical Engineers, Atlanta, August 8–11, 1993, pp. 35–43.
[3] J.C. Chai, H.S. Lee, S.V. Patankar, Treatment of irregular geometries using a Cartesian coordinates finite-volume radiation heat transfer procedure, Numer. Heat Transfer B Fund. 26 (1994) 225–235.
[4] H.-M. Koo, R. Vaillon, V. Goutiere, V.L. Dez, H. Cha, T.-H. Song, Comparison of three discrete ordinates methods applied to two-dimensional curved geometries, Int. J. Thermal Sci. 42 (2003) 343–359.
[5] H.-M. Koo, K.-B. Cheong, T.-H. Song, Schemes and applications of first and second-order discrete ordinates interpolation methods to irregular two-dimensional geometries, J. Heat Transfer 119 (1997) 730–737.
[6] G. Parthasarathy, H.S. Lee, J.C. Chai, S.V. Patankar, Monte Carlo solutions for radiative heat transfer in irregular two-dimensional geometries, J. Heat Transfer 117 (1995) 792–794.
[7] M. Sakami, A. Charette, Application of a modified discrete ordinates method to two-dimensional enclosures of irregular geometry, J. Quant. Spectrosc. Radiat. Transfer 64 (2000) 275–298.
[8] F.L. Meng, F. McKenty, R. Camarero, Radiative heat transfer by the discrete transfer method using an unstructured mesh, in: ASME HTD, vol. 2044, 1993, pp. 55–56.

[9] W.M.G. Malalasekera, E.H. James, Radiative heat transfer calculations in three-dimensional complex geometries, J. Heat Transfer 118 (1996) 225–228.
[10] W.M.G. Malalasekera, F.C. Lockwood, Computer simulation of the King's cross fire: effect of radiative heat transfer on fire spread, in: Proceedings of Institute of Mechanical Engineers, vol. 205, 1991, pp. 201–208.
[11] P. Talukdar, S.C. Mishra, Transient conduction and radiation heat transfer with heat generation in a participating medium using the collapsed dimension method, Numer. Heat Transfer A Appl. 39 (2001) 79–100.
[12] S.C. Mishra, P. Talukdar, D. Trimis, F. Durst, Computational efficiency improvements of the radiative transfer problems with or without conduction-a comparison of the collapsed dimension method and the discrete transfer method, Int. J. Heat Mass Transfer 46 (16) (2003) 3083–3095.
[13] P. Mahanta, S.C. Mishra, Collapsed dimension method applied to radiative transfer problems in complex enclosures with participating medium, Numer. Heat Transfer B Fund. 42 (4) (2002) 367–388.
[14] S.V. Patankar, Numerical Heat Transfer and Fluid Flow, Hemisphere, Washington, DC, 1980.
[15] S.C. Mishra, A novel computational approach for the solution of radiative heat transfer problems in participating media, PhD thesis, IIT Kanpur, India, 1997.
[16] J.C. Chai, G. Parthasarathy, H.S. Lee, S.V. Patankar, Finite volume radiation heat transfer procedure for irregular geometries, J. Thermophys. Heat Transfer 9 (3) (1995) 410–415.